

pointing "down" relative to the mean ring plane, as is the equatorial C2 hydroxyl, places constraints on the likely orientations of the O2 near neighbors. In this context, it is worth noting that, for all of the pyranoid pentose and hexose sugars, which exist predominantly in the 4C_1 conformation, the preferred anomer in aqueous solution is that form which has the anomeric, O1 hydroxyl and the O2 hydroxyl groups on opposite sides of the mean plane of the ring,⁵⁵ as is the case in β -D-glucopyranose. Since the free energy difference between the two forms in water at 300 K is only

(55) Shallenberger, R. S. *Advanced Sugar Chemistry*; AVI Publishing Co.: Westport, CT, 1982.

approximately 0.34 kcal/mol, it is probable that if this difference is due to solvation effects, much longer simulations will be necessary for such a small difference to emerge from the background statistical noise of the data.

Acknowledgment. I thank M. Karplus, S. N. Ha, L. Madsen, B. R. Brooks, and Tran Vinh for helpful discussions. This work was supported in part by NIH Grant No. GM34970 and by Hatch Project 143-7433, USDA. Figures 3 and 17 were prepared using the HYDRA molecular graphics program written by R. E. Hubbard of the University of York.

Registry No. α -D-Glucopyranose, 492-62-6.

Early Stages of Diborane Pyrolysis: A Computational Study

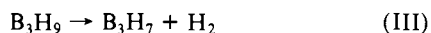
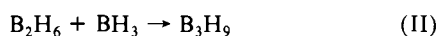
John F. Stanton,^{*,†,‡} William N. Lipscomb,[†] and Rodney J. Bartlett[§]

Contribution from the Gibbs Chemical Laboratory, Harvard University, Cambridge, Massachusetts 02138, and Quantum Theory Project, Departments of Chemistry and Physics, University of Florida, Gainesville, Florida 32611. Received November 25, 1988

Abstract: Methods of many-body perturbation theory and the coupled-cluster approximation are applied to a study of two elementary processes believed to play a role in the pyrolysis of diborane, $BH_3 + B_2H_6 \rightarrow B_3H_9$ (II) and $B_3H_9 \rightarrow B_3H_7 + H_2$ (III). Results indicate that the reaction pathway for II proceeds through a transition state stabilized by a donation-backdonation interaction reminiscent of that involved in hydroboration and that the activation and reaction enthalpies (at 400 K) for this process are approximately 14 and -5 kcal/mol, respectively. Loss of molecular hydrogen from the triborane(9) formed in II appears to occur with a negligible kinetic barrier, leading to an isomer of B_3H_7 with C_{2v} symmetry. Significantly, a C_s form of triborane(7) is found to be 4 kcal/mol more stable than the C_{2v} isomer. Thus, the theoretical reaction enthalpy for III of +9 kcal/mol represents an approximate upper limit to the activation energy for the most favorable route of hydrogen loss from B_3H_9 , suggesting that the barrier for this process is much lower than has heretofore been assumed. This result, coupled with the probability that triborane(9) is formed with ≈ 20 kcal/mol of excess internal energy, casts doubt over the common belief that step III is the slow step in the uncatalyzed pyrolysis of diborane. Relative rates for thermolysis of B_2H_6 and B_2D_6 are also computed from the theoretical energies, harmonic force fields, and structures. Regardless of which step is assumed to be rate-determining, resulting values of k_H/k_D (1.7 and 2.4 for II and III, respectively) are substantially smaller than the observed ratio of ≈ 5 . Possible sources of this discrepancy are discussed.

I. Introduction

The thermal interconversion of the boranes is an extremely complex process. Although direct pyrolysis of diborane was used by Stock in the 1920's to synthesize a number of larger boron hydrides,¹ little is known about the individual reactions which participate in this process. Nearly forty years after the first kinetic studies appeared in the literature,² even the initial steps of the reaction sequence have not been clearly established. Exemplary studies by the groups of Schaeffer³ and Fehlner⁴ have produced evidence which suggests that the overall conversion is initiated by the symmetric dissociation of diborane, followed by addition of a borane fragment to unreacted diborane with subsequent elimination of molecular hydrogen.



The kinetics of this process are 3/2 order in diborane, implicating either II or III as the rate-determining step,² with respective rate expressions

$$\text{Rate} = k_{11}K_1^{1/2}[B_2H_6]^{3/2} \quad (1)$$

and

$$\text{Rate} = k_{111}K_{11}K_1^{1/2}[B_2H_6]^{3/2} \quad (2)$$

where K_j is the equilibrium constant for reaction j . When perdeuterated diborane is pyrolyzed, a very large retardation of the rate is observed ($k_H/k_D \approx 5$).^{3a} Since vibrational contributions to energy differences typically favor products of unimolecular dissociations and are necessarily smaller (in magnitude) for reactions involving perdeuterated species, one would expect a larger value of k_H/k_D if III is the slowest step under the reaction conditions, as pointed out by Enrione and Schaeffer.^{3a} Effective activation enthalpies for B_2H_6 pyrolysis can be deduced from eq 1 and 2 and are

$$H_{\text{eff}}^* = 0.5\Delta H_1^* + H_{11}^* \quad (3)$$

if II limits the rate and

$$H_{\text{eff}}^* = 0.5\Delta H_1^* + \Delta H_{11}^* + H_{111}^* \quad (4)$$

if loss of molecular hydrogen from triborane(9) is the slow step.

(1) Stock, A. *Hydrides of Boron and Silicon*, Cornell University Press: Ithaca, NY, 1933.

(2) Early kinetic studies of diborane pyrolysis are summarized in the following: *Production of the Boranes and Related Research*, Holzmann, R. T., Ed.; Academic Press: New York, 1967; pp 90-115. More recent studies are referenced in the following: Greenwood, N. N.; Greatrex, R. *Pure Appl. Chem.* **1987**, *59*, 857.

(3) (a) Enrione, R. E.; Schaeffer, R. *Inorg. Nucl. Chem.* **1961**, *18*, 103. (b) Brennan, G. L.; Schaeffer, R. *Inorg. Nucl. Chem.* **1961**, *20*, 205.

(4) Fehlner, T. P. In *Boron Hydride Chemistry*; Muettterties, E. L., Ed.; Academic Press: New York, 1975; pp 175-196, and references therein.

[†]Harvard University.

[‡]AT&T Foundation Fellow.

[§]University of Florida.

Table I. Cartesian Coordinates (in bohrs) of the Optimized (321/21)MBPT(2) Structures Used in the Present Research^a

BH ₃			B ₂ H ₆			TS2					
x	y	z	x	y	z	x	y	z			
B	0.0000	0.0000	0.0000	0.0000	1.6822	B	-2.0689	-1.3056	0.0350		
H	0.0000	0.0000	2.2607	0.0000	-1.6822	B	-0.5299	1.9665	0.0325		
H	1.9579	0.0000	-1.1304	1.8504	0.0000	B	2.5772	-0.6697	0.0182		
H	-1.9579	0.0000	-1.1304	H	-1.8504	0.0000	H	0.1211	-0.6569	-1.0113	
				H	0.0000	1.9785	2.7583	H	2.8340	1.6266	0.0262
				H	0.0000	1.9785	-2.7583	H	-2.9541	0.9320	0.1213
				H	0.0000	-1.9785	2.7583	H	-2.0718	-2.3020	2.0393
				H	0.0000	-1.9785	-2.7583	H	-2.8536	-2.2307	-1.8659
								H	-0.3385	2.8405	2.0894
								H	-0.5658	3.1573	-1.8738
								H	2.7225	-1.7276	1.9936
								H	3.2138	-1.5954	-1.9476

B ₃ H ₉			B ₃ H ₇ (C _{2v})			B ₃ H ₇ (C _s)					
x	y	z	x	y	z	x	y	z			
B	0.0000	2.2013	0.0522	B	0.0000	0.0000	2.0450	B	0.0496	1.6894	0.0000
B	1.9064	-1.1007	0.0522	B	0.0000	1.6530	-0.9575	B	0.0496	-0.8546	1.9114
B	-1.9064	-1.1007	0.0522	B	0.0000	-1.6530	-0.9575	B	0.0496	-0.8546	-1.9114
H	2.0735	1.1972	-0.8118	H	0.0000	0.0000	-2.8254	H	-1.3433	1.3874	2.0028
H	-2.0735	1.1972	-0.8118	H	1.9537	2.7884	-1.0608	H	-1.3433	1.3874	-2.0028
H	0.0000	-2.3943	-0.8118	H	1.9537	-2.7884	-1.0608	H	1.3496	3.5072	0.0000
H	0.0000	2.9067	2.1780	H	-1.9537	2.7884	-1.0608	H	-1.4805	-2.4688	2.2158
H	0.0000	3.7309	-1.6273	H	-1.9537	-2.7884	-1.0608	H	-1.4805	-2.4688	-2.2158
H	2.5173	-1.4534	2.1780	H	0.0000	1.9271	3.2095	H	1.7766	-0.6227	3.3491
H	-2.5173	-1.4534	2.1780	H	0.0000	-1.9271	3.2095	H	1.7766	-0.6227	3.3491
H	3.2311	-1.8655	-1.6273								
H	-3.2311	-1.8655	-1.6273								

^aThe equilibrium bond length of H₂ at this level of theory is 1.3986 bohr.

Unfortunately, the intermediates involved in the presumed pyrolysis sequence are highly reactive; the Lewis acid B₃H₇ has been found only in adducts,⁵ a "triboron hydride" has been observed by mass spectroscopy,⁶ and BH₃ has also proven to be elusive. Indeed, the first unambiguous observation of the vibrational spectrum of any of these species appeared just recently, when Hirota and co-workers studied the out-of-plane bending mode of BH₃.⁷ Due to the short lifetimes of the triboron hydrides, it is very difficult to learn much about the mechanisms of the elementary processes from experimental studies. Consequently, theoretical calculations may be able to provide some insight into this interesting and important reaction system.

Recent quantum chemical studies⁸ of the symmetric dissociation of diborane (reaction I above) have yielded dissociation energies which are in excellent agreement with the experimental value of 36 ± 3 kcal/mol⁹ and have suggested that the process proceeds along a C_{2h} reaction pathway with a negligible kinetic barrier,^{8c} again in accord with the experimental activation energy of -1 ± 2 kcal/mol for the self-association of borane.¹⁰ Combined with the experimental effective activation energy for B₂H₆ pyrolysis of ≈27 kcal/mol² and theoretical studies which indicate that reaction II is approximately thermoneutral,¹¹ eq 3 and 4 indicate that the activation enthalpy associated with the rate-determining step is in the vicinity of 10 kcal/mol.

By contrast to the well-understood and relatively uncontroversial reaction I, essentially nothing is known about the mechanism of either of the reactions involving triborane(9). Indeed, it is not at all obvious that low-energy pathways should exist for either

process; the addition of BH₃ to diborane involves steric interference by one of the bridging hydrogens in B₂H₆, and the elimination of hydrogen from B₃H₉ involves the breaking of two chemical bonds. Preliminary studies of these reactions have been carried out by McKee and Lipscomb,¹² who found activation barriers of 22.4 (II) and 12.6 (III) kcal/mol. Although both values are higher than the ≈10 kcal/mol barrier expected for the rate-determining step, the calculations were not performed at a sufficiently high level to warrant a detailed comparison with experiment. Furthermore, subsequent work has demonstrated that the structure used to evaluate the activation energy for II is actually a second-order saddle point on the B₃H₉ potential surface¹³ and that the true activated complex has no elements of symmetry.¹⁴

In this paper, we report results of a high-level theoretical study of reactions II and III. We investigate the reaction pathway for both processes, optimizing structures of the ground states and activated complexes for reactions II and III (the transition states will hereafter be referred to as TS2 and TS3, respectively) at the level of many-body perturbation theory (MBPT)¹⁵, and go on to calculate the associated thermochemical parameters and isotope effects. In addition to providing the groundwork for further investigation in this area, we hope that the present work (along with the more recent theoretical studies of reaction I in the literature⁸) will help others gain a greater understanding of the reactions involved in the pyrolysis process.

II. Computational Details

Most of the calculations reported in this paper used the ACES program system, developed by Bartlett and collaborators.¹⁶ Final optimi-

(5) Some of the structures and chemistry of B₃H₇-L adducts are presented in the following: Shore, S. G. In *Boron Hydride Chemistry*; Muetterties, E. L., Ed.; Academic Press: New York, 1975; pp 132-134.

(6) Fridmann, S. A.; Fehlner, T. P. *J. Am. Chem. Soc.* **1971**, *93*, 2824.

(7) Kawaguchi, K.; Butler, J. E.; Yamada, C.; Bauer, S. H.; Minowa, T.; Kanomori, K.; Hirota, E. *J. Chem. Phys.* **1987**, *87*, 2438.

(8) (a) Page, M.; Adams, G. F.; Binkley, J. S.; Melius, C. F. *J. Phys. Chem.* **1987**, *91*, 2675. (b) Stanton, J. F.; Bartlett, R. J.; Lipscomb, W. N. *Chem. Phys. Lett.* **1987**, *138*, 525. (c) DeFrees, D. J.; Raghavachari, K.; Schlegel, H. B.; Pople, J. A.; Schleyer, P. v. R. *J. Phys. Chem.* **1987**, *91*, 1857.

(9) Fehlner, T. P.; Mappes, G. W. *J. Phys. Chem.* **1969**, *73*, 873.

(10) Mappes, G. W.; Fridmann, S. A.; Fehlner, T. P. *J. Phys. Chem.* **1970**, *74*, 3307.

(11) (a) Ortiz, J. V.; Lipscomb, W. N. *Chem. Phys. Lett.* **1983**, *103*, 59.

(b) Stanton, J. F.; Lipscomb, W. N.; Bartlett, R. J.; McKee, M. L. *Inorg. Chem.* **1989**, *28*, 109.

(12) This research is summarized in the following: Lipscomb, W. N. *Pure Appl. Chem.* **1983**, *55*, 1431.

(13) Stanton, J. F.; Lipscomb, W. N. unpublished results.

(14) The early searches for TS2 were conducted under the assumption that the ground state of B₃H₉ had D_{3h} symmetry. Subsequent work, however, revealed that the D_{3h} structure was unstable with respect to distortion to C_{3v} symmetry (McKee, M. L.; Lipscomb, W. N. *Inorg. Chem.* **1985**, *24*, 2317) ruling out the possibility of an activated complex with a plane of symmetry.

(15) Bartlett, R. J. *Ann. Rev. Phys. Chem.* **1981**, *32*, 359 and references therein.

(16) Bartlett, R. J.; Purvis, G. D.; Fitzgerald, G. B.; Harrison, R. J.; Lee, Y. S.; Laidig, W. D.; Cole, S. J.; Trucks, G. W.; Salter, E. A.; Magers, D. H.; Sosa, C.; Rittby, M.; Pal, S.; Stanton, J. F. ACES (Advanced Concepts in Electronic Structure)—an ab initio program system.

Table II. Harmonic Frequencies for BH₃, B₂H₆, TS2, and the Two Isomers of B₃H₇ Considered in the text^b

BH ₃		B ₂ H ₆		TS2		B ₃ H ₇ (C _{2v})		B ₃ H ₇ (C _s)	
1185	2622	411	1240	134	1181	321	1127	317	1160
1253 ^a	2761 ^a	816	1801	216	1199	447	1243	431	1254
		817	1922	246	1207	476	1243	665	1293
		888	1975	273	1246	616	1287	748	1391
		936	2214	501	1868	619	1859	749	1521
		996	2679	624	2153	658	2122	774	2184
		1033	2691	771	2283	830	2654	838	2246
		1108	2784	776	2500	934	2674	890	2697
		1239	2795	861	2669	949	2728	951	2711
				949	2684	994	2739	1017	2803
				1028	2731	994	2751	1021	2815
				1076	2783	1086	2816	1136	2819
				1105	2814				
				1116	2875				
				1168	679i				

^aFrequencies correspond to doubly degenerate normal coordinates. ^bValues for B₃H₇ were obtained from SCF harmonic force fields calculated with the (321/2) basis; remaining frequencies were computed from the 3-21G MBPT(2) force field.

zations for all systems considered in this research were performed at the MBPT(2) level, using the [3s2p1d]/[2s1p] [hereafter referred to as (321/21)] basis of ref 17. Cartesian coordinates of all structures are collected for reference in Table I. Preliminary optimizations were carried out with two smaller basis sets: the 3-21G set of Binkley et al.¹⁸ and a [3s2p1d]/[2s] [(321/2)] basis derived from the (321/21) set by removal of the hydrogen polarization functions. Since our previous experience with the ground state of triborane(9)^{11b} suggested that geometries obtained with the (321/21) and (321/2) basis sets would be very similar, the smaller of the two was used to generate initial guesses for the significantly more costly final optimizations. Transition structures were located by two different approaches: the eigenvector following (EF) algorithm presented by Baker¹⁹ (as implemented in the ACES optimization routine) and the Newton-Raphson (NR) search incorporated into Gaussian 86.²⁰ For TS3, the 3-21G transition structure of McKee and Lipscomb²¹ served as an appropriate starting guess for further optimizations, and the NR method performed well. The structure of the transition state for reaction II, however, has proven to be an especially frustrating problem and has been a subject of investigation in this group for many years. Due to overestimation of the relative stability of BH₃ in SCF calculations, even the gross features of the B₃H₉ potential energy hypersurface are qualitatively in error at this level of theory: as one boron is displaced from the equilibrium structure of B₃H₉ and moved away from the remaining borons, the SCF minimum energy pathway eventually becomes dissociative with respect to three BH₃ units. When correlation is included at the simplest MBPT(2) level, the dissociation energy for this channel rises from 9.7 to 52.0 kcal/mol.^{11b} Hence, to be meaningful, the geometry of TS2 must be located at the correlated level. The solution to this problem is further complicated by transition-state symmetry rules, which force the activated complex for reaction II to have no elements of symmetry. Consequently, thirty degrees of conformational freedom need to be simultaneously optimized.

To search for TS2, we chose to start with the C_s second-order saddle point found by McKee and Lipscomb. Since the NR method is only suited for cases in which the guess structure is at a point where the curvature of the potential surface is appropriate,²² the EF algorithm was used. The initial optimization was performed at the 3-21G MBPT(2) level of theory, where the analytic force constants were available. After only 13 cycles, the transition search converged. The performance of the method in this application (where there is a large number of adjustable

parameters and where the starting guess is poor) is remarkable and suggests that the EF scheme may be appropriate for even more complex problems. After convergence, the 3-21G MBPT(2) Hessian was evaluated and used to search the (321/2) MBPT(2) surface for TS2. Again, the EF method converged rapidly to a stationary point. All of these calculations were performed on a Digital Equipment Co. VAX station 3200 microcomputer. The expensive MBPT(2) optimization using the (321/21) basis was carried out with the NR method, by using the Cray version of Gaussian 86 at the Pittsburgh Supercomputing Center. As expected, the (321/2) and (321/21) structures are very similar, and TS2 was found after only two cycles of optimization.

To estimate the thermodynamic and kinetic parameters for both reactions, calculations were carried out on the (321/21) MBPT(2) structures at higher levels of MBPT and with various implementations of the coupled-cluster (CC) approximation.²³ While the (321/21) and a larger [4s3p1d]/[3s1p] [(431/31)]¹⁷ basis were used in the MBPT calculations, only the smaller of the two was used in the CC studies. MBPT correlation energies were determined at third and fourth order [MBPT(3) and MBPT(4)] and at the SDQ-MBPT(4) level, in which the contributions of triply excited determinants are neglected. CC theory is an infinite order generalization of MBPT based on the so-called exponential *ansatz*

$$|\Psi\rangle = e^T|0\rangle \quad (5)$$

The exponential excitation operator, which maps a reference (here, SCF) wave function ($|0\rangle$) into an exact eigenstate of the Hamiltonian ($|\Psi\rangle$), can be subdivided into a product of exponential cluster operators corresponding to particular levels of excitation [$e^T = e^{T_1+T_2+T_3+\dots+T_n}$]. Although a full CC calculation (where n is equal to the number of particles) is not practical for most problems of chemical interest, excellent approximations to the correlation energy and wave function can usually be achieved if T is simplified in an appropriate manner. In this research, two well-tested models have been used: the CCSD scheme ($T = T_1 + T_2$),²⁴ which is the infinite order generalization of SDQ-MBPT(4), and CCSD + T (CCSD),²⁵ in which T (CCSD) is the first-order perturbative correction to the CCSD energy. In cases where the standard molecular orbital electronic configuration makes the only major contribution to the exact wave function, the economical CCSD + T (CCSD) model is an accurate approximation to the very expensive and sophisticated CCSDT scheme,²⁶ which is the infinite-order counterpart of MBPT(4). For such well-behaved systems, CCSD + T (CCSD) correlation energies are usually within 1% of the exact (full CI or full CC) basis set correlation energies.²⁷

Quadratic force fields used to calculate the harmonic vibrational frequencies presented in the next section were obtained analytically using the ACES program package. SCF frequencies computed with the (321/2) basis set for BH₃, B₂H₆, and B₃H₉ are documented in ref 11b, while corresponding values for two isomers of B₃H₇ are listed in Table II. Because of the special nature of TS2, harmonic frequencies for this

(17) Redmon, L. T.; Purvis, G. D.; Bartlett, R. J. *J. Am. Chem. Soc.* **1979**, *101*, 2856.

(18) Binkley, J. S.; Pople, J. A.; Hehre, W. J. *J. Am. Chem. Soc.* **1980**, *102*, 939.

(19) Baker, J. *J. Comput. Chem.* **1986**, *7*, 385.

(20) Frisch, M. J.; Binkley, J. S.; Schlegel, H. B.; Raghavachari, K.; Melius, C. F.; Martin, R. L.; Stewart, J. J. P.; Bobrowicz, F. W.; Rohlfing, C. M.; Kahn, L. R.; DeFrees, D. J.; Seeger, R.; Whiteside, R. A.; Fox, D. J.; Fleuder, E. M.; Pople, J. A. *Gaussian 86*; Carnegie-Mellon Quantum Chemistry Publishing Unit: Pittsburgh, PA, 1986.

(21) McKee, M. L.; Lipscomb, W. N., unpublished research.

(22) By appropriate, we mean that the Hessian matrix evaluated at the initial point in configuration space should have the correct number of eigenvalues: 1 for a transition state search, and 0 when a local minimum is sought. Unlike the NR approach, which will converge to any nearby stationary point regardless of its Hessian index, the EF scheme can be made to follow one eigenvector uphill to a stationary point, while all others (regardless of the sign of their associated eigenvalues) are followed downhill.

(23) Bartlett, R. J.; Dykstra, C. E.; Paldus, J. In *Advances Theories and Computational Approaches to the Electronic Structure of Molecules*; Dykstra, C. E., Ed.; Reidel: Dordrecht, 1983.

(24) Purvis, G. D.; Bartlett, R. J. *J. Chem. Phys.* **1982**, *76*, 1910.

(25) Urban, M.; Noga, J.; Cole, S. J.; Bartlett, R. J. *J. Chem. Phys.* **1985**, *83*, 4041.

(26) Noga, J.; Bartlett, R. J. *J. Chem. Phys.* **1987**, *86*, 7041.

(27) (a) Lee, Y. S.; Bartlett, R. J. *J. Chem. Phys.* **1984**, *80*, 4371. (b) Lee, Y. S.; Kucharski, S. A.; Bartlett, R. J. *J. Chem. Phys.* **1985**, *81*, 5906; **1985**, *82*, 5761. (c) Cole, S. J.; Bartlett, R. J. *J. Chem. Phys.* **1987**, *86*, 873.

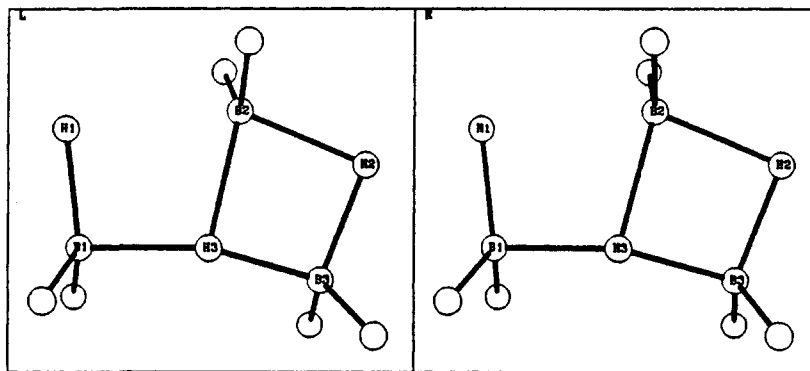


Figure 1. Stereoview of the transition state for reaction II (TS2). Coordinates correspond to the (321/21)-MBPT(2) saddle point, and the atomic designations are consistent with the discussion in section III of the text.

Table III. Selected Internal Coordinates for TS2, Optimized at the MBPT(2) Level with Various Basis Sets^b

	3-21G	(321/2)	(321/21)
$r(\text{B}_1\text{-B}_2)$	2.44	2.15	2.16
$r(\text{B}_1\text{-B}_3)$	2.57	2.47	2.48
$r(\text{B}_2\text{-B}_3)$	2.01	1.91	1.91
$r(\text{B}_1\text{-H}_1)$	1.22	1.23	1.22
$r(\text{B}_2\text{-H}_1)$	1.94	1.79	1.79
$r(\text{B}_3\text{-H}_1)$	3.01	3.02	3.02
$r(\text{B}_1\text{-H}_2)$	3.13	3.06	3.05
$r(\text{B}_2\text{-H}_2)$	1.31	1.40	1.40
$r(\text{B}_3\text{-H}_2)$	1.30	1.28	1.27
$r(\text{B}_1\text{-H}_3)$	1.46	1.42	1.41
$r(\text{B}_2\text{-H}_3)$	1.87	1.55	1.53
$r(\text{B}_3\text{-H}_3)$	1.28	1.33	1.33
Δ^a	0.47	0.57	0.55

^aDistance between H₃ and the plane formed by the boron atoms.

^bThe atomic designations are consistent with those in Figure 1. All distances are in Å.

structure were obtained analytically at the MBPT(2) level.²⁸ These values, calculated with the 3-21G basis, are also listed as well as those computed at the same level for BH₃ and B₂H₆. Thermodynamic parameters were calculated from the theoretical minimum energy structures and the scaled harmonic frequencies²⁹ by the standard methods of statistical thermodynamics in the ideal gas, rigid-rotor, harmonic oscillator approximation. The signs of energy differences reported in this paper follow the usual thermodynamic convention, and all values refer to the ¹¹B isotopomers.

III. Results

A. B₂H₆ + BH₃ → B₃H₉. A.1. Structure of the Transition State. Internal coordinates for TS2 optimized at the MBPT(2) level with the various basis sets are listed in Table III. The eigenvector (in the Cartesian representation) which corresponds to the imaginary harmonic frequency for this structure is documented in Table IV. The existence of a single negative Hessian eigenvalue (that associated with the transition vector) proves that this is a true transition state on the 3-21G MBPT(2) potential surface, and an inspection of the reaction coordinate shows that it does indeed correspond to reaction II. We point out, however, that we have made no attempt to calculate the quadratic force fields of the (321/2) or (321/21) structures. Due to the lack of symmetry in TS2 and the relatively large number of basis functions, these calculations would require a substantial amount of

Table IV. Contributions of Individual Atomic Motions to the Normal Coordinate Corresponding to the Transition Vector for Reaction II

	x	y	z
B	0.0911	-0.0634	-0.0105
B	-0.1029	-0.0022	0.0234
B	-0.0065	0.0699	-0.0057
H	-0.1075	0.1513	-0.0340
H	0.3001	0.4675	-0.1221
H	0.3084	-0.3239	-0.0174
H	-0.0007	0.0093	0.0100
H	0.0662	-0.0960	0.0491
H	-0.0223	-0.2141	-0.0012
H	-0.0301	0.0071	-0.0063
H	-0.1020	-0.0128	0.0249
H	-0.2115	-0.0354	0.0192
Transition State Structure			
B	-1.8830	2.6360	0.0000
B	-1.0979	-1.9017	0.0000
B	2.1958	0.0000	0.0000
H	1.3503	-2.3098	0.0979
H	0.3078	1.2061	-0.9005
H	-3.4158	0.9240	0.2469
H	2.8033	0.5354	2.0944
H	3.6088	-0.0447	-1.7599
H	-1.9498	-2.4670	1.9923
H	-1.8678	-2.4451	-2.0295
H	-1.2260	3.6366	1.9091
H	-1.9815	3.6757	-2.0086

^aThe mass-weighting has been removed from the eigenvector, and the values listed correspond to the pure Cartesian displacements with respect to the 3-21G MBPT(2) saddle point structure listed at the bottom of the table. Coordinates of the saddle point structure are in atomic units, and the atomic ordering corresponds to the numbering scheme in Figure 1.

computer time. Hence, we are not able to conclusively show that these structures represent transition states. Nevertheless, the similarity of the three structures suggests that this is the case. It is also important to note that the qualitative differences between the (321/21) MBPT(2) and 3-21G MBPT(2) structures parallel those between fully polarized and split-valence MBPT(2) equilibrium structures of B₃H₉. Hence, we will assume that the (321/2) and (321/21) stationary points are the transition states for reaction II in the space spanned by the respective basis sets.

The most obvious effect of increasing the basis set size is the contraction of boron-boron distances in the activated complex. This shortening parallels that found for the ground-state structure of triborane(9)^{11b} (although it is somewhat less dramatic in TS2), indicating that this may be a general feature of the global B₃H₉ potential surface. Also remarkable is the large distance between the plane formed by the three boron atoms and the hydrogen which corresponds to the bridging proton of B₂H₆ nearest the attacking BH₃. This atom, which must undergo significant displacement during the course of the reaction, is 0.55 Å out of the B-B-B plane, suggesting that the steric blockage caused by this bridging hydrogen is largely responsible for the activation energy of reaction

(28) Methods used for MBPT(2) second derivative evaluation in the ACES program system (see ref 16) are described in the following: Harrison, R. J.; Fitzgerald, G. B.; Laidig, W. D.; Bartlett, R. J. *Chem. Phys. Lett.* **1986**, *124*, 291. Handy, N. C.; Amos, R. D.; Gaw, J. F.; Rice, J. E.; Simandras, E. D.; Lee, T. J.; Harrison, R. J.; Laidig, W. D.; Fitzgerald, G. B.; Bartlett, R. J. In *Geometrical Derivatives of Energy Surfaces and Molecular Properties*; Jorgensen, P.; Simons, J., Eds.; Reidel: Dordrecht, 1986; p 179.

(29) A scale factor of 0.90 was chosen for the (321/21)-SCF frequencies, while a value of 0.93 was applied to those calculated from the 3-21G MBPT(2) force field. These empirical factors are chosen to account (in an approximate way) for inadequacies in the theoretical force field as well as differences between the actual fundamental frequencies and those computed from the exact quadratic force field.

Table V. Theoretical Bare Barrier Heights (ΔE^\ddagger) and Reaction Energies (ΔE^R) for the Reaction $\text{BH}_3 + \text{B}_2\text{H}_6 \rightarrow \text{B}_3\text{H}_9$ Calculated at Various Correlated Levels with the (321/21) and (431/31) Basis Sets^d

	ΔE^\ddagger		ΔE^R ^a	
	(321/21)	(431/31)	(321/21)	(431/31)
SCF	29.1	31.1	11.4	13.9
MBPT(2) ^b	11.6	13.4	-11.1	-9.0
MBPT(2) ^c	11.1		-12.1	
MBPT(3)	13.4	15.1	-8.7	-6.6
SDQ-MBPT(4)	14.3	15.9	-7.4	-5.4
MBPT(4)	12.2	13.6	-9.7	-7.9
CCSD	14.7	16.3	-6.8	-4.8
CCSD+T(CCSD)	12.4	13.8	-9.3	-7.5

^a These values were originally documented in ref 11b.

^b Configurations with vacant K-shell orbitals not included. ^c Calculated with full configuration space. ^d All values in kcal/mol. CC calculations with the [4s3p1d]/[3s1p] basis were estimated; see text.

II. From the stereoview of TS2 in Figure 1, one can see that the attacking BH_3 unit forms an apparent donor-acceptor interaction with the B_2H_6 substrate. While the proximal bridging hydrogen of diborane (H_3) is donated to the attacking boron atom (B_1), the $\text{B}_1\text{-H}_1$ bond is properly situated to join in the incipient $\text{B}_2\text{-H}_1\text{-B}_1$ three-center two-electron bond. Significantly, the two bridging hydrogens of diborane have moved nearer B_3 in the transition state, leading to a net polarization of the B_2H_6 fragment toward something resembling $^{\delta-}\text{H}_2\text{BH}_2\text{-BH}_2^{\delta+}$. The attacking boron of BH_3 is much closer to the "electronegative" end of the perturbed B_2H_6 molecule, and the first part of the reaction mechanism (the uphill path from reactants) appears to largely involve transfer of H_3 from the bridging position in diborane toward one of the three (equivalent) three-center bonds in the product. Beyond the transition state, the electropositive nature of B_2 is moderated by the formation of the $\text{B}_2\text{-H}_1\text{-B}_1$ three-center two-electron bond as well as by movement of H_2 away from B_3 toward a symmetric position.

Qualitatively, TS2 resembles a point on the BH_3 /ethylene hydroboration pathway.³⁰ In reaction II, the incoming BH_3 interacts with one of the terminal borons and the electron density in the (protonated) "double-bond" of diborane. The attack of B_1 on the apparently electronegative region of the weakly polarized B_2H_6 molecule is consistent with the anti-Markownikoff addition of BH_3 to substituted olefins,³¹ and the donation-backdonation mechanism parallels that found in molecular orbital studies of hydroboration. Nevertheless, this comparison can only be taken so far—the analogy is complicated by the steric interference of the proximal proton (H_3) of diborane and by possible direct interaction between boron atoms in the transition state. As we noted in our study of triborane(9),^{11b} electron correlation effects are especially important in this molecule and appear to introduce significant interactions between the nominally nonbonded boron atoms. These direct $\text{B}\cdots\text{B}$ effects may play an important role in the stabilization of B_3H_9 and greatly complicate the picture of bonding. Consequently, there may also be important boron-boron interaction in the activated complex. If this is true, a description of the process in terms of density donated from a "hydridic" H_3 (to be compared to the electronegative carbon center in hydroboration) toward B_1 would not be appropriate. Taken together, this interaction and any $\text{B}_1\cdots\text{B}_3$ "bond" formation in the transition state is analogous to the formation of the B-C bond in hydroboration. Similarly, the counterpart of the (complete) hydride transfer in hydroboration is the subsequent formation of the remaining bridge bond ($\text{B}_1\text{-H}_1\text{-B}_2$), which can be viewed as a partial hydride transfer to the electropositive part of the B_2H_6 substrate.

A.2. Energetics. Table V lists theoretical values for the vibrationless barrier height (ΔE^\ddagger) and energy change (ΔE^R) for

reaction II. Because of the large number of basis functions and the lack of symmetry in TS2, the K-shell molecular orbitals (chiefly linear combinations of the boron 1s atomic orbitals) were constrained to be doubly occupied in all correlated calculations. With the larger basis, determinants involving excitation to the three highest lying virtual functions ($\epsilon > 18$ au) were also omitted. The magnitude of the systematic error caused by this approximation can be estimated from the table, which contains results of (321/21)MBPT(2) calculations carried out with both the full and constrained configuration spaces. Differences between the corresponding values of ΔE^\ddagger and ΔE^R are surprisingly large; correlation effects involving core electrons appear to be considerably greater in " B_3H_9 " (both TS2 and the equilibrium structure) than in the separated monomers. The error in the bare barrier height (0.55 kcal/mol) is somewhat smaller than the 1.0 kcal/mol error found for the reaction energy, suggesting that correlation of core electrons is greatest in the B_3H_9 ground state.

Although CC calculations were not performed with the larger (431/31) basis, barrier heights and reaction energies were estimated by assuming that the difference between these values and their fourth-order MBPT counterparts (see section II) are the same as those obtained with the (321/21) basis. In view of the relatively small difference between the CC and MBPT(4) results calculated with the smaller basis, we feel that the infinite-order effects included in the two CC models are relatively unimportant in the present example. This has been a persistent feature in CC/MBPT studies of the boron hydrides;^{8b,11,32} in all cases, the MBPT expansion of the correlation energy appears to be well converged at fourth order, while the MBPT(4) and CCSD+T(CCSD) [as well as SDQ-MBPT(4) and CCSD] reaction energies differ by only a fraction of a kcal/mol. Another common feature in our studies of the boranes is the order-by-order dependence of calculated energy differences. With no exception, the simplest MBPT(2) approximation appears to overestimate the contribution of electron correlation: the best calculations [MBPT(4) or CCSD+T(CCSD)] produce values which are intermediate between MBPT(2) and SDQ-MBPT(4). Consequently, it appears that the relatively inexpensive MBPT(4) model is capable of recovering from most of the inadequacies of the SCF description for these systems. Unlike problematic molecules in which more than one electronic configuration makes a large contribution to the exact wave function, the electronic structure of the boron hydrides seems to be consistently well-described by a single configuration. The correlation effects which are so important in the boranes arise from relatively weak mixing of a large number of excited configurations into the wave function. Such situations, which are said to involve "dynamic" correlation, are easily and effectively treated with the finite-order MBPT models.

A close inspection of Table V reveals a nearly parallel correlation dependence of the predicted reaction energy and barrier height for reaction II. As the level of theory is improved, each increment to ΔE^\ddagger and ΔE^R has the same sign; the magnitude of the changes are somewhat larger for ΔE^R in all cases. Consequently, it is apparent that the ground state of B_3H_9 is stabilized by correlation to a greater extent than is TS2. Indeed, the (431/31) SCF and MBPT(4) activation energies for the reverse reaction ($\text{B}_3\text{H}_9 \rightarrow \text{B}_2\text{H}_6 + \text{BH}_3$) are 17.2 and 21.5 kcal/mol, respectively. Possibly, the preferential stabilization of the equilibrium structure might be due to its shorter $\text{B}\cdots\text{B}$ distances, which result in potentially enhanced boron-boron interactions. While the somewhat revolutionary view that direct interactions between nominally nonbonded boron atoms play an important role in boron chemistry is an enticing area for speculation and further research, no definitive conclusions can be drawn at this time. In the future, we plan to study the correlation dependence of the electron density in the boranes. At that time, we hope to be able

(30) (a) Dewar, M. J. S.; McKee, M. L. *Inorg. Chem.* **1978**, *17*, 1075. (b) Clark, T.; Schleyer, P. v. R. *J. Organomet. Chem.* **1978**, *156*, 191. (c) Sundberg, K. R.; Graham, G. D.; Lipscomb, W. N. *J. Am. Chem. Soc.* **1979**, *101*, 2863.

(31) Brown, H. C.; Rao, B. C. S. *J. Am. Chem. Soc.* **1959**, *81*, 6423.

(32) (a) Stanton, J. F.; Lipscomb, W. N.; Bartlett, R. J. *Proceedings of IMEBORON VII*; World Scientific: Singapore, 1988; pp 74-82. (b) Stanton, J. F.; Bartlett, R. J.; Lipscomb, W. N. In *Molecules in Chemistry, Physics and Biology*; Marauini, J., Ed.; Elsevier: Amsterdam, 1988. (c) Stanton, J. F.; Lipscomb, W. N.; Bartlett, R. J., submitted to *J. Am. Chem. Soc.*, following paper in this issue.

Table VI. Coordinates (in bohrs) for Structures of TS3 Found at the 3-21G SCF and (321/2)MBPT(2) Levels of Theory^a

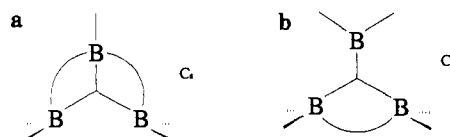
3-21G SCF			(321/2)MBPT(2)		
Coordinates					
B	2.0435	0.0000	B	2.0160	0.0000
B	-1.0926	-1.8925	B	-1.0138	-1.7560
B	-1.0089	1.7474	B	-0.9954	1.7241
H	-2.7573	0.3673	H	-2.8691	0.4860
H	1.3465	-2.3283	H	1.4635	-2.3695
H	0.4887	2.1997	H	0.3880	2.2598
H	3.0975	0.5041	H	3.0673	0.5600
H	3.2461	-0.1074	H	3.2173	-0.0033
H	-1.9714	-2.5438	H	-1.9135	-2.4611
H	-1.6263	-1.9469	H	-1.5724	-2.8273
H	-1.2574	3.0571	H	-1.2287	3.2154
H	-1.3560	2.9500	H	-1.3270	2.8819
Transition Vector					
B	0.0227	0.0255		-0.0269	
B	-0.0384	-0.0041		0.0038	
B	-0.0188	0.0585		-0.0348	
H	0.1627	-0.2474		0.0089	
H	-0.0707	0.0781		-0.0494	
H	0.5147	-0.4392		0.3765	
H	-0.0330	0.0399		-0.0118	
H	0.0947	-0.0992		0.0303	
H	0.0321	-0.0583		0.0081	
H	0.0130	-0.0431		0.0096	
H	0.0101	-0.1201		0.0988	
H	-0.3463	0.0163		0.1615	

^a Also included is the 3-21G SCF transition vector.

to objectively assess the relative importance of B...B "bonding" and to gain physical insight into the curious effects we have observed in these systems.

B. $B_3H_9 \rightarrow B_3H_7 + H_2$. Unlike TS2, an activated complex for reaction III is easily located at the SCF level (the search is complicated only by the large number of conformational degrees of freedom due to the lack of symmetry). The 3-21G coordinates and associated transition vector are listed in Table VI. An inspection of the structure (in Table I) and the reaction coordinate clearly shows that the initial product of dissociation is the C_{2v} isomer of triborane(7) pictured in Figure 2. This is an important observation, since a number of high-level theoretical studies have indicated that this is not the lowest energy form of B_3H_7 .^{11a,33} Consequently, the kinetically and thermodynamically favored products of dissociation may not be the same in this case.

In order to study this system in more detail, we have carried out optimizations of the transition structure and selected isomers of B_3H_7 at the correlated level and have performed calculations at the same levels of theory used in the study of reaction II. Following the strategy used in the substantially more difficult searches for TS2, the initial optimization was performed with the (321/2) basis at the MBPT(2) level, using the analytic 3-21G Hessian and the NR search in Gaussian 86. This structure, which is also included in Table VI, is considerably more compact than that obtained with the 3-21G basis but retains the same qualitative features. When hydrogen polarization functions were included in the basis, the NR optimization oscillated wildly and did not converge. An analysis of the reaction pathway using the EF scheme showed that the kinetic barrier obtained at the lower levels of theory is spurious—addition of H_2 to the C_{2v} structure of B_3H_7 appears to occur *without activation*. The apparent absence of a kinetic barrier in this process is not so surprising when the reverse reaction is considered. Within the molecular orbital approximation (which remains useful as a descriptive tool despite its demonstrated limitations in the triboron hydrides), the boron in B_3H_7 which eventually accepts the terminal hydrogen has a formally vacant p orbital. The reaction pathway appears to be stabilized by an unsymmetrical Lewis acid–base adduct in which H_2 donates density to the unoccupied orbital of B_3H_7 . The free BH_2 group

**Figure 2.** The two isomers of B_3H_7 considered in the present study.**Table VII.** Theoretical Reaction Energies for $B_3H_9 \rightarrow B_3H_7 (C_{2v})$ (I) + H_2 and for $B_3H_7 (C_{2v}) \rightarrow B_3H_7 (C_s)$ (II) Calculated at Various Correlated Levels with the (321/21) and (431/31) Basis Sets^a

	I		II	
	(321/21)	(431/31)	(321/21)	(431/31)
SCF	3.3	2.2	1.3	0.7
MBPT(2)	14.7	14.2	-3.7	-4.7
MBPT(3)	14.2	13.7	-3.1	-4.0
SDQ-MBPT(4)	13.5	13.0	-2.7	-3.6
MBPT(4)	14.3	14.0	-3.3	-4.4
CCSD	12.9	12.4	-2.5	-3.5
CCSD+T(CCSD)	13.9	13.5	-3.1	-4.2

^a All values in kcal/mol.

(see Figure 2) eventually undergoes a complex rotation (no elements of symmetry are present at any nonterminal point on the minimum energy path), as one of the hydrogens moves into a bridging position with respect to an adjacent boron. As the reaction proceeds, the H...H distance in " H_2 " is increased by slightly more than 1 Å; one of the two protons of the attacking hydrogen molecule ends up as part of a B–H–B three-center two-electron bond in triborane and as an adjacent terminal hydrogen which is "cis" to the bridging hydrogens (with respect to the plane of the boron atoms). We should point out that addition of H_2 to BH_3 also appears to occur without activation.^{32c} The apparent absence of a kinetic barrier for addition to BH_3 and B_3H_7 may be a general feature of $H_2 + B_nH_m$ reactions, where the boron hydride is a Lewis acid with one or more formally vacant orbitals.

Theoretical reaction energies for the formation ($B_3H_9 \rightarrow B_3H_7[C_{2v}] + H_2$) and isomerization ($B_3H_7[C_{2v}] \rightarrow B_3H_7[C_s]$) of B_3H_7 are listed in Table VII. Results obtained for the isomerization confirm those found previously: the global minimum on the B_3H_7 surface appears to be the C_s structure, with the C_{2v} form about 4 kcal/mol higher in energy. Consequently, if there is a pathway addition of H_2 to the C_s isomer with a low barrier, the dissociation channel leading to the C_{2v} form may be effectively closed, and the corresponding dissociation energy would only be an approximate upper limit to the activation energy of the most favorable process. Hence, on the basis of our calculations, we cannot be sure whether the C_s or C_{2v} isomer of B_3H_7 is the initial product of reaction III, nor can we rule out the possibility that a mixture of both is generated.

A more involved study of B_3H_7 , including investigation of the pathways for hydrogen addition to the C_s form and the mechanism and barrier of the isomerization, is beyond the scope of the present research and is currently underway in our laboratory. Results will be reported in the future.

C. Enthalpies of Activation and Isotope Effects. Using the (321/21) MBPT(2) structures and the theoretical harmonic frequencies listed in Table II, vibrational and thermal corrections to the bare barrier heights and reaction energies were computed. Energy differences at absolute zero (ΔE_0) and at a typical pyrolysis temperature of 400 K are listed in Table VIII as well as enthalpy, entropy, and Gibbs free energy differences at 400 K. Also included are the corresponding values for reactions involving the perdeuterated species.

The assumption that either II or III is the slowest step in the sequence yields a rate expression which is 3/2 order in diborane (as observed experimentally), with the effective activation enthalpies given by eq 3 and 4. Since it is not possible to unambiguously determine the rate-determining step from the experimental rate law and effective activation energy alone, both alternatives must be considered. Use of the parameters listed in Table VIII leads to predicted effective enthalpies of activation of 32.1 (assuming step II is slowest) and 22.6 (step III slowest)

Table VIII. Thermodynamic and Kinetic Parameters for Reactions I, II and III, Involving the Undeuterated and Perdeuterated Species^a

	undeuterated species	perdeuterated species
Reaction I ($B_2H_6 \rightarrow 2BH_3$)		
ΔE_c	39.9	39.9
ZPC	-6.2	-4.7
ΔE_o	33.7	35.3
ΔH (400 K)	35.9	37.0
ΔG (400 K)	21.8	22.4
Reaction II ($B_2H_6 + BH_3 \rightarrow B_3H_9$)		
ΔE_c	-7.5	-7.5
ZPC	4.0	2.9
ΔE_o	-3.5	-4.6
ΔH (400 K)	-4.6	-5.3
ΔG (400 K)	8.7	8.2
ΔE_c^*	13.8	13.8
ZPC	1.1	0.7
ΔE_o^*	14.9	14.5
ΔH^* (400 K)	14.2	14.1
ΔG^* (400 K)	25.3	25.5
Reaction III ($B_3H_9 \rightarrow B_3H_7 (C_{2v}) + H_2$)		
ΔE_c	13.5	13.5
ZPC	-6.3	-4.4
ΔE_o	7.2	9.1
ΔH (400 K)	9.2	10.8
ΔG (400 K)	-2.4	-1.6
Reaction IV ($B_3H_7 (C_{2v}) \rightarrow B_3H_7 (C_s)$)		
ΔE_c	-4.2	-4.2
ZPC	0.3	0.3
ΔE_o	-3.9	-3.9
ΔH (400 K)	-4.1	-4.2
ΔG (400 K)	-4.2	-4.2

^aAll values based on the estimated (431/31) CCSD+T(CCSD) electronic energy differences and the (321/21) MBPT(2) structures. Vibrational corrections for reactions I and III are based on the (321/2) SCF harmonic force field, while those for II are derived from the 3-21G MBPT(2) force constants.

kcal/mol. Since the CCSD+T(CCSD) model is exact through fourth-order MBPT and includes many contributions which occur at MBPT(5) and higher orders,³⁴ neglect of these residual electron correlation contributions to the barrier heights for II and III probably results in only a small error (≈ 1 kcal/mol). Two other effects, however, could be more important in the present case. First, expansion of the basis beyond the (431/31) set might change the predicted barrier heights by as much as 5 kcal/mol.³⁵ Second, the unusual correlation and basis set dependence of the minimum energy structure of B_3H_9 ^{11b} suggests that the geometries of both TS2 and the triborane(9) ground state may not be well converged at the (321/21) MBPT(2) level. If this is true, energies calculated with the actual equilibrium and saddle point geometries might result in somewhat different barrier heights. A conservative estimate of the uncertainty associated with the theoretical values of ΔH_{eff}^* is < 7 kcal/mol. Unfortunately, neither of the two points raised above can be addressed at present. The lack of symmetry in TS2 makes use of very large basis sets virtually impossible; even the relatively small (431/31) set requires the evaluation, storage, and transformation of 1.7×10^7 integrals, a significant number even for modern supercomputers. Furthermore, transition-state searches at higher orders of MBPT, while possible, would be prohibitively expensive.

Although both values for the effective activation enthalpy given above are in reasonable agreement with the experimental range of measurements, the relative barrier heights of the *individual* steps II and III suggest that III could not be the rate-limiting step in the *uncatalyzed* pyrolysis of B_2H_6 . Indeed, even if the activation

energy for II is overestimated and is actually smaller than that for step III, entropy considerations suggest that the rate constant for the unimolecular process (III) will be much larger. Assuming a frequency factor of 10^{14} s^{-1} , which is typical of four-center elimination reactions such as III³⁶ and the "upper limit" ΔH^* of 9 kcal/mol, the rate constant expected for III at 420 K is found to be $\approx 10^9 \text{ s}^{-1}$. This calculation, however, assumes that triborane(7) and hydrogen are formed from B_3H_9 in thermal equilibrium. An inspection of the potential energy profile for reactions II and III, however, suggests that this may not be the case. Since TS2 lies about 20 kcal/mol above the ground state of triborane(9), B_3H_9 will be formed with a large excess of internal energy. At low-to-moderate pressures, the rate of cooling via collisional deactivation might then be much slower than the elimination of hydrogen, and the actual rate constant for reaction III could be considerably larger than the simple prediction of 10^9 s^{-1} expected for decomposition of *ground-state* triborane. In fact, since TS2 lies ≈ 10 kcal/mol above the *products* of reaction III, it is entirely possible that this step occurs so rapidly that for all practical purposes the formation of B_3H_7 might be best represented by the following direct reaction: $B_2H_6 + BH_3 \rightarrow B_3H_7 + H_2$.

In contrast to the elimination of hydrogen from the most stable form of triborane(9), steps I and II appear to be relatively slow processes. From a kinetic study of reaction I,¹⁰ we know that the rate constant for dissociation of diborane is $\approx 10^{-3} \text{ s}^{-1}$ at 400 K, while application of transition-state theory to reaction II results in a predicted k of $\approx 10^0 \text{ M}^{-1} \text{ s}^{-1}$. Since the (barrierless) self-association of borane should be much faster than reaction II, the concentration of BH_3 under the reaction conditions is approximately $(K_1[B_2H_6])^{1/2}$. At pressures typically employed in pyrolysis studies (100–300 Torr), $[BH_3] \approx 10^{-7} \text{ M}$ and the overall rate of reaction II is expected to be much slower than I. Hence, the addition of BH_3 to B_2H_6 probably represents the rate-limiting step during the early stages of diborane pyrolysis.

Since the conclusion reached above contradicts the commonly invoked assumption that the rate of diborane pyrolysis is limited by step III, some discussion of the evidence supporting the established view is warranted. First, we point out that our predicted rate constant for B_3H_9 formation is approximately 10^7 smaller than that measured for the formation of a "triborane" from B_2H_6 and BH_3 .³⁷ Unfortunately, the product of this reaction was identified only by mass spectroscopy and could have been *any* triborane (B_3H_x). Fehlner³⁸ has pointed out that the measured rate might have corresponded to formation of a weak adduct of B_2H_6 and BH_3 which may or may not rearrange to the ground state of B_3H_9 and lead to further reaction. Clearly, a theoretical investigation of plausible metastable complexes between diborane and borane would be desirable, as would be further experimental work in this area. Another justification for assignment of III as rate-limiting has been the observation that diborane pyrolysis appears to be inhibited by addition of H_2 into the reaction mixture.² Although this inhibition would be expected if hydrogen elimination is involved in the rate-determining step, some effects of the reverse of reactions I–III may occur even if II is mainly controlling the rate. Also, addition of H_2 might result in the formation of BH_5 , effectively reducing the concentration of BH_3 and consequently the rate of reaction II. A recent theoretical study^{32c} has shown that BH_5 is ≈ 3 kcal/mol more stable than BH_3 and H_2 , indicating that this complex may play a more important role in boron hydride chemistry than previously believed. Finally, the assumption that the unimolecular reaction III is slower than the bimolecular addition of borane to diborane is often rationalized by associating the former reaction with the loss of hydrogen from tetraborane(10) (B_4H_{10}), for which an activation energy of 24 kcal/mol has been determined experimentally.^{3b} It has been customary to assume that a comparable barrier exists for reaction III. If this were the case and step II were indeed the very fast bimolecular formation

(34) For a discussion of the various CC approximations and their relationship to many-body perturbation theory, see: Kucharski, S. A.; Bartlett, R. J. *Adv. Quant. Chem.* **1986**, *18*, 281.

(35) See, for example: Hehre, W. J.; Radom, L.; Schleyer, P. v. R.; Pople, J. A. *Ab Initio Molecular Orbital Theory*; Wiley: New York, 1986.

(36) Benson, S. W. *Thermochemical Kinetics*; J. W. Wiley and Sons: New York, 1976; p 111.

(37) Fridmann, S. A.; Fehlner, T. P. *Inorg. Chem.* **1972**, *11*, 936.

(38) Fehlner, T. P., personal communication.

Table IX. Theoretically Determined Values of k_H/k_D for the Initial Stages of Diborane Pyrolysis, Assuming Either Step II or III is Rate-Limiting

rate-limiting step ^a	k_H/k_D
II	1.73
III	2.35

^a Reaction II is the addition of BH_3 to diborane, while III is the loss of molecular hydrogen from triborane(9) (see text).

of a triborane observed by Fridmann and Fehlner, then III would probably be the slow step in the sequence. Unfortunately, our theoretical barrier height of 9 kcal/mol indicates that loss of hydrogen from triborane occurs much more rapidly than the analogous elimination from tetraborane(10). Hence, even if the rate of II suggested by our calculations is in considerable error, it is not likely that this process can occur rapidly enough to compete with step III under the reaction conditions. A plausible explanation for the apparently different propensities of B_3H_9 and B_4H_{10} to lose H_2 can be traced to the structures of the two compounds. In triborane(9), the bridge hydrogens are shared equally by the two nearest boron atoms and are only 1.79 Å³⁹ away from the "cis" terminal hydrogens with which they join to form H_2 along the reaction pathway. On the other hand, the bridging hydrogens are not shared equally in tetraborane(10) but rather are more strongly bonded to B_1 and B_3 (the borons which are connected by a formal B–B bond) and are more than 2 Å from both protons of the nearest terminal BH_2 group. Hence, to form the most likely initial product of H_2 elimination, a strongly bound bridge hydrogen [$r_{B_1-H_6} = 1.17$ Å (X-ray)⁴⁰, 1.24 Å (theory)⁴¹] must move a large distance away from B_1 in order to join in the formation of an H–H bond. This is probable source of the rather high barrier for this process, compared to reaction III.

As mentioned in the introduction, the pyrolysis of diborane exhibits a strong deuterium isotope effect ($k_H/k_D \approx 5$),^{3a} and this observation has also been used to justify the assignment of reaction III as the rate-limiting step. Although the calculated *electronic* thermodynamic and kinetic parameters for reactions I–III are not isotopically dependent by virtue of the Born–Oppenheimer approximation, contributions of the vibrational and rotational energies lead to different values of the energy differences for isotopomers. Using transition state theory, the isotopic dependence of the rate for this process can be estimated from

$$k_H/k_D = [K_I(H)/K_I(D)]^{1/2} e^{-[\Delta G^\ddagger_{II}(H) - \Delta G^\ddagger_{II}(D)]/RT} \quad (6)$$

or

$$k_H/k_D = [K_I(H)/K_I(D)]^{1/2} [K_{II}(H)/K_{II}(D)] e^{-[\Delta G^\ddagger_{III}(H) - \Delta G^\ddagger_{III}(D)]/RT} \quad (7)$$

where reactions II and III, respectively, have been assumed rate-limiting. Resulting values are documented in Table IX. In our calculations, we have assumed that reaction III proceeds with no kinetic barrier, and consequently use the theoretical equilibrium structures of the dissociation products at infinite separation as the "transition-state" geometry. While this may not be entirely appropriate, the true transition structure is likely to be very loose, and the approximation afforded by the present treatment should be adequate for at least a crude estimation of the isotope effect. We should point out that the values in Table VIII suggest that B_2H_6 is dissociated to a greater extent than B_2D_6 under typical

(39) This distance is taken from the (321/21) MBPT(2) minimum energy structure.

(40) Nordman, C. E.; Lipscomb, W. N. *J. Am. Chem. Soc.* **1953**, *75*, 4116. A microwave study supporting nearly equal B–H₆ distances of 1.43 Å [Simmons, N. P. C.; Burg, A. B.; Beaudet, R. A. *Inorg. Chem.* **1981**, *20*, 533] has also appeared, but these authors acknowledged difficulties in determining the coordinates of the bridging hydrogen atoms and conjectured that these atoms undergo large amplitude vibrational motions. We believe that the large asymmetry of B–H₆ distances found in both the X-ray and theoretical structure determinations are actual features of both the equilibrium structure.

(41) McKee, M. L.; Lipscomb, W. N. *Inorg. Chem.* **1981**, *20*, 4452.

pyrolysis conditions [K_H/K_D (400 K) = 2.0], in contradiction to the prediction of Enrione and Schaeffer^{3b} but in agreement with a more recent calculation which predicted a similar K_H/K_D (360 K) of 2.5.^{32b}

Regretably, invocation of neither II nor III as the rate-limiting step results in a kinetic isotope effect in satisfactory agreement with the experimental value. Barring the existence of a qualitatively different lower energy transition state for II, it does not appear that the reaction sequence I–III can be reconciled with the magnitude of the rate reduction when B_2D_6 is heated, provided (1) the reactions occur *homogeneously* and (2) that quantum tunneling makes a negligible contribution to the rate. Note, however, that both qualifications apply only to reaction II. Only negligible kinetic barriers are associated with both I and III; therefore neither catalysis nor tunneling can lead to significant rate enhancements for these two reactions. Consequently, if the experimental measurement of k_H/k_D is accurate and the reaction scheme I–III is correct, the rate of addition of BH_3 to diborane at ≈ 360 K⁴² may include a substantial contribution from proton tunneling.

IV. Discussion

On the basis of the results presented in this paper, it appears likely that the addition of BH_3 to diborane represents the rate-limiting step during the early stages of *uncatalyzed* diborane pyrolysis. This is only a tentative conclusion, however, because it is based upon two important premises. First, we tacitly assume that reactions I–III are the important steps leading from B_2H_6 to the higher boranes and that products of possible (reversible) side reactions such as $BH_3 + H_2 \rightarrow BH_5$ and $BH_3 + B_2H_6 \rightarrow B_2H_6 \cdots BH_3$ do not lead to further reaction but only revert to the constituents of the respective complexes. Another factor to be considered is whether TS2 is truly the lowest transition state for II. Considering the very complicated 30-dimensional B_3H_9 energy surface, it would be difficult to rule out the possibility of a lower energy transition state for this process. However, the gross features of the TS2 structure in Figure 1 are exactly those which we had anticipated by appealing to chemical intuition, and there are no obvious alternative candidates. Since the pyrolysis of diborane is fundamental to the field of boron hydride chemistry, we sincerely hope that the conclusion of the present study will stimulate further experimental and theoretical investigation of this complex reaction system.

Also uncertain is the kinetically favored product of reaction III. If the C_{2v} isomer is formed initially, the minimum energy pathway passes through configurations similar to the (spurious) (321/2) MBPT(2) transition structure in Table VI, and there is little or no kinetic barrier. Addition of hydrogen to the C_s isomer of triborane(7) to produce the C_{3v} form of B_3H_9 probably involves substantial molecular rearrangement and likely occurs with a moderate activation energy. If the height of the barrier is 4 kcal/mol or less, however, the C_s isomer might be the predominant dissociation product. Nevertheless, it is certain that the ΔH^\ddagger calculated for the decomposition to the C_{2v} isomer serves as an *upper limit* to the theoretical barrier height of the lowest energy dissociation, and we have succeeded in demonstrating the existence of a low-energy pathway for loss of H_2 from triborane(9).

If TS2 is correct, the mechanism of II is qualitatively similar to two other addition reactions of BH_3 —the self-association reaction to form diborane and the ethylene– BH_3 hydroboration reaction. The donation–backdonation process appears to be important in all three reactions and may be a ubiquitous feature in the chemistry of the boron hydrides, as postulated many years ago.⁴³ Unlike reaction II, however, the self-association and hydroboration reactions occur with little or no activation barrier. As discussed above, the source of the barrier for II likely involves the steric interference of the bridging hydrogen of B_2H_6 nearest the attacking boron atom, unlike the other two processes in which very little intrareactant nuclear displacement occurs along the

(42) The experiments of ref 3a were carried out over a range of temperatures from 341–361 K.

(43) Lipscomb, W. N. *Science* **1977**, *196*, 1047.

reaction pathway. Consequently, the addition reactions of BH_3 may be divided into (at least) two categories: those in which the substrate is a Lewis acid with vacant or electron-deficient p orbitals (in hydroboration, this would correspond to the ylid resonance form of ethylene), and others in which the substrate must undergo significant nuclear rearrangement to form a donation-backdonation interaction. In the former case, which only involves polarization of the electron cloud (a relatively low-energy process), the associated activation energies are likely to be very small, while the latter class of additions would typically have higher barriers. Future studies in boron hydride chemistry, both theoretical and

experimental, should serve to judge the propriety of this operational classification.

Acknowledgment. This work was supported by the National Science Foundation under Grant CHE85-15347 and the Office of Naval Research. Early stages of the research were conducted while one of us (R.J.B.) was visiting Harvard University as a Guggenheim Fellow. We are also grateful for a generous allocation of computing time at the NSF-supported Pittsburgh Supercomputing Center.

Registry No. 2BH_3 , 19287-45-7.

A Theoretical Investigation of the Structure and Properties of BH_5

John F. Stanton,^{*,†,‡} William N. Lipscomb,[†] and Rodney J. Bartlett[§]

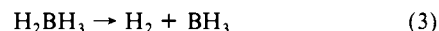
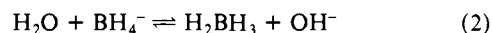
Contribution from the Gibbs Chemical Laboratory, Harvard University, Cambridge, Massachusetts 02138, and Quantum Theory Project, Departments of Chemistry and Physics, University of Florida, Gainesville, Florida 32611. Received November 25, 1988

Abstract: The intermolecular complex between borane (BH_3) and molecular hydrogen is studied with methods based on many-body perturbation theory and the coupled-cluster approximation. Calculations with very large Gaussian basis sets indicate that BH_5 is particularly stable, with the minimum of the intermolecular potential roughly 6 kcal/mol below that of the separated monomers. A pronounced basis set dependence is observed; highly correlated CCSD+T(CCSD) calculations with an unpolarized $[3s2p]/[2s]$ basis set suggest a totally repulsive intermolecular interaction, while the singly polarized $[3s2p1d]/[2s1p]$ basis predicts a binding energy of 2.7 kcal/mol. Continued expansion of the basis is found to systematically increase the stability of this system. The structures of four isomers are optimized at the MBPT(2)- $[3s2p1d]/[2s1p]$ level and are compared with results of previous theoretical studies of BH_5 and its organic analogue CH_5^+ . Of these isomers, only a C_s structure with the H_2 subunit eclipsing one of the B-H bonds of BH_3 is found to be a minimum—another C_s and a C_{2v} structure are found to be transition states for internal rotation and hydrogen scrambling, while a C_{4v} isomer is a second-order saddle point on the potential surface. MBPT(2) vibrational frequencies and infrared band intensities are also evaluated for the equilibrium structure and are analyzed in terms of interacting molecular subunits. The theoretical enthalpic barriers for dissociation and internal rearrangement at 298 K are 2.4 and 6.6 kcal/mol, respectively. Rate calculations using a modified RRKM model which permits an approximate inclusion of quantum effects suggest that proton tunneling may play a significant role in the experimentally observed hydrogen scrambling process. Overall, the results are qualitatively consistent with the participation of BH_5 in the aqueous hydrolysis of tetrahydroborate anion.

I. Background

Early studies of the aqueous hydrolysis of the borohydride anion¹ led to general agreement that (1) molecular hydrogen was evolved stepwise, with the release of the first mole representing the rate-determining step; (2) mixed hydroxyborohydride intermediates $[\text{BH}_{4-n}(\text{OH})_n]^-$ were involved; and (3) the reaction was catalyzed by acid. Initially, it was believed that the rate-determining formation of borane (BH_3) was a single elementary process involving a formally neutral activated complex between hydronium ion and BH_4^- . This view was eventually challenged by Mesmer and Jolly², who found that although most of the hydrogen evolved from hydrolysis of BH_4^- in D_2O is HD, a statistically significant amount of H_2 is released as well. To account for this observation, these authors proposed an intermediate with stoichiometry BH_4D , which principally decomposes to yield HD but also produces small quantities of H_2 . Further evidence against the simple one-step mechanism was produced 10 years later by Kreevoy and Hutchins,³ who studied BH_4^- hydrolysis over a pH range from 10.7 to 13.6. A plot of the pseudo-first-order rate constant vs pH was highly nonlinear, implicating a process with a qualitatively different rate law. Also confirmed was a previous observation

that borohydride takes up deuterium when hydrolysis is carried out in strongly basic D_2O . Although this finding could account for evolution of D_2 during hydrolysis via the postulated one-step mechanism, it does not satisfactorily explain the small amount of H_2 seen by Mesmer and Jolly.² To explain the experimental observations, Kreevoy and Hutchins postulated the following mechanism for the production of borane. The rate law derived



from these elementary reactions is successful in fitting the observed pH dependence: in acidic or weakly basic solutions, the simple pseudo-first-order rate law is recovered, but the exchange with solvent [the reverse of reaction (2)] competes at high pD, and the slope $d(\text{rate})/d(\text{pD})$ decreases dramatically, in excellent qualitative

(1) Gardiner, J. A.; Collat, J. W. *Inorg. Chem.* **1965**, *4*, 1208. Gardiner, J. A.; Collat, J. W. *J. Am. Chem. Soc.* **1965**, *87*, 1692. David, R. E.; Bromels, E. B.; Kibby, C. L. *J. Am. Chem. Soc.* **1962**, *84*, 885. Mochalov, K. N.; Gil'manchin, C. G. *Dokl. Akad. Nauk. SSSR* **1960**, *132*, 134. David, R. E.; Swain, C. G. *J. Am. Chem. Soc.* **1960**, *82*, 5949.

(2) Mesmer, R. E.; Jolly, W. L. *J. Am. Chem. Soc.* **1962**, *84*, 2039.

(3) Kreevoy, M. M.; Hutchins, J. E. C. *J. Am. Chem. Soc.* **1972**, *94*, 6371.

[†] Harvard University.

[‡] AT&T Foundation Fellow.

[§] University of Florida.